

# SECONDARY PARTICLES IN THE ACCELERATION STAGE OF HIGH CURRENT, HIGH VOLTAGE NEUTRAL BEAM INJECTORS: THE CASE OF THE INJECTORS OF THE THERMONUCLEAR FUSION EXPERIMENT ITER\*

G. Serianni<sup>#</sup>, P. Agostinetti, V. Antoni, M. Cavenago<sup>1</sup>, G. Chitarin,

G. Fubiani<sup>2</sup>, E. Gazza, N. Marconato, N. Pilan, P. Veltri

Consorzio RFX, Euratom-ENEA Association, C.so Stati Uniti 4, I-35127, Padova, Italy

<sup>1</sup> INFN/LNL, Legnaro (PD) Italy

<sup>2</sup> CNRS, LAPLACE, F-31062 Toulouse, France.

## Abstract

The thermonuclear fusion experiment ITER requires a 33 MW auxiliary heating power from two Neutral Beam Injectors (HNB), each of them providing 40 A of negative deuterium ions. The EU activities oriented to the realisation of a negative ion electrostatic accelerator for the HNB comprise the construction in Padova of SPIDER, a test bed devoted to the optimisation of the beam source. The secondary particles which are generated inside the SPIDER accelerator are the subject of the present contribution.

## INTRODUCTION

Within the European effort towards the realisation of the neutral particle injectors for ITER based on negative ion acceleration, the activities oriented to the optimisation of the electrostatic accelerator comprise the construction in Padova of SPIDER, a facility devoted to the optimisation of the beam source [1]. SPIDER is a negative ion accelerator designed for [2] 100 keV acceleration voltage and 40/60 A (deuterium/hydrogen) beam current. The is constituted of three grids (Figure 2) [3]: the grid facing the plasma (Plasma Grid, PG), through which extraction of negative ions takes place, the Extraction Grid (EG); and the Grounded Grid (GG).

The development activities recently carried out at Consorzio RFX resulted in an optimised final design of the accelerator [4]; the main innovations are: a magnetic filter in the ion source produced solely by a suitable arrangement of electrical currents, featuring also a very low magnetic field outside the source [5]; deflection out of the beam of the electrons co-extracted with the negative ions by means of permanent magnets located in the EG; compensation of the corresponding deflection of negative ion trajectories by means of permanent magnets and ferromagnetic material in the GG; the latter helps also to reduce the long-range magnetic field downstream of the accelerator.

The work presented here regards the numerical modelling and characterisation of secondary particles in the optimised SPIDER accelerator. Three types of particles are considered: neutrals, generated by stripping

of negative ions; positive ions, produced by double stripping of negative ions or by ionisation of the background gas; electrons produced by impact of particles on the grids, stripped from negative ions inside the accelerator, and generated by ionisation of the background gas.

The investigation is performed by means of the EAMCC code [6], which is a 3D relativistic particle tracking code where macroparticle trajectories, in prescribed electrostatic and magnetostatic fields, are calculated inside the accelerator. Inputs to the code are the electric and magnetic fields inside the accelerator; collisions are described using a Monte-Carlo method and represent electron and heavy ion/neutral collisions with grids, single and double stripping reactions of negative ions and ionisation of the background gas. Two separate simulations are carried out, for extracted negative ions and for co-extracted electrons, respectively.

The reference condition corresponds to the following parameters [4]: extracted H<sup>-</sup> current density: 355 A/m<sup>2</sup>; electron-to-negative-ion extracted current density ratio: 1; electrostatic field: evaluated with SLACCAD [7] and magnetic field evaluated with OPERA [8] and ANSYS [9]; gas pressure: 0.3 Pa inside the RF source and 0.05 Pa downstream of the GG; beam temperature: 0.18 eV. The code computes the corresponding currents and heat deposited on the various grids by secondary particles as well as their spatial distribution.

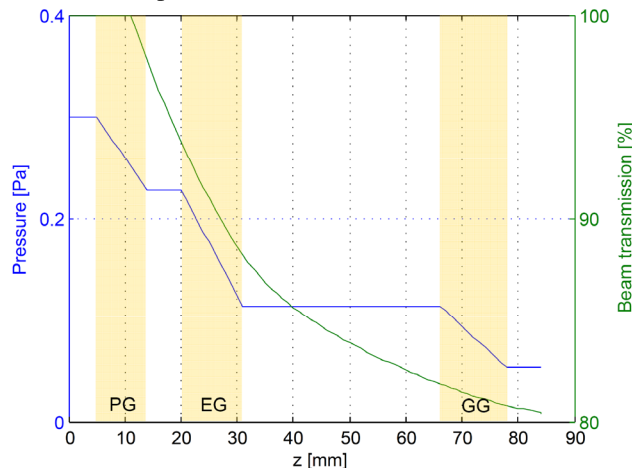


Figure 1: Profile of gas pressure and beam transmission.

\* Work set up in collaboration and financial support of Fusion for energy

<sup>#</sup> gianluigi.serianni@igi.cnr.it

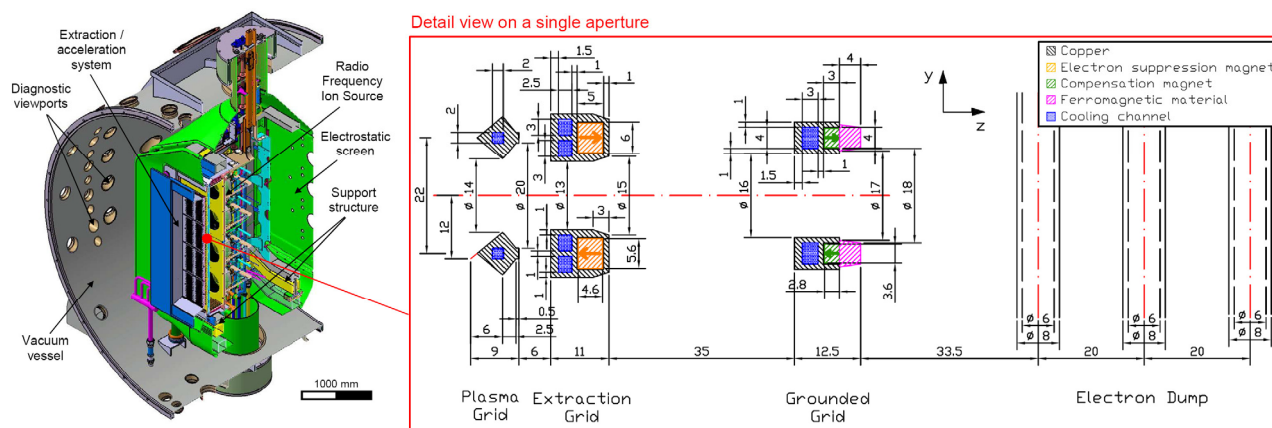


Figure 2: Section view of the updated SPIDER Extractor/Accelerator system and Electron Dump.

## SECONDARY PARTICLES IN SPIDER

The generation of secondary particles affects the electric field profile, since the current associated to the negative ions is partially transformed via stripping into electron current (Figure 1), which has a much lower space charge density.

Stripping and ionisation generate neutrals and positive ions, which may hit the surface of the grids as their trajectories are not subjected to the whole electric field profile. Consequently, heat and current are deposited on the grids, as given in Table 1. Except for the last row of the table, all other quantities are due to secondary particles; the indices “str” and “coext” refer to the electrons generated during the simulation of negative ions or of co-extracted electrons respectively.

Specifically, positive ions are quite collimated in the centre of the apertures and are accelerated backwards; they impact on the back-plate of the ion source, depositing highly localised energy flux, though the total power associated to them is not high (100 kW).

At the accelerator exit all types of particles can be found; specifically, the effect of stripping results in a high power associated to neutral hydrogen (330 kW).

Again electrons are responsible for the majority of the power deposited on the grids; in particular, the effectiveness of the suppression field is demonstrated by the huge power ( $\sim 0.7$  MW) deposited on the EG.

## MANAGEMENT OF ACCELERATED ELECTRONS

In terms of power and current deposited on the grids, the main secondary particles in SPIDER are the electrons, issuing from stripping of negative ions, generated from ionisation of the background gas or emitted when other particles hit a material surface. As already described, such electrons are accelerated by the electrical field and they can either deposit their power on the various surfaces of the accelerator or run across the accelerator and exit the GG apertures.

It is clear that the major contribution to the power deposited on the grids is due to electrons; specifically, co-extracted electrons give essentially the whole load on the EG, whereas the power reaching the GG is equally shared between stripping and co-extracted electrons.

Table 1: Distribution of power in the accelerator.

surface	particles	power [kW]	current [A]
exit to source	$H^+ / H_2^+$	10 / 90	0.2 / 1.6
EG	$e_{str} / e_{coext}$	30 / 636	4.5 / 64.8
GG	$e_{str} / e_{coext}$	252 / 218	3.2 / 2.2
accel. exit	$e_{str} / e_{coext}$	330 / 170	7.1 / 1.9
accel. exit	$H^0 / H^+$	330 / 10	- / 0.2
accel. exit	$H^-$	5720	57.2

Another result of the simulations is that about 0.5 MW is associated to the electrons exiting the accelerator. Such electrons shall be dumped in a controlled way to avoid damages to material surfaces. Several electron dumping methods have been proposed [10]. For SPIDER a preference has been granted to the solution presented in Figure 2, consisting of three arrays of tubes surrounding each aperture of the GG [11].

To compute the trajectories of electrons and the associated heat deposited on the Electron Dump (ED) the EDAC code (Electron Dump Accountancy Code) has been developed at Consorzio RFX in the MATLAB® environment. The code performs the following operations: it receives from EAMCC the accelerator geometry and the position/velocity of particles at a plane 20 mm downstream of the accelerator exit (where the space charge is expected to be compensated); it extends the trajectories until they hit an ED tube or the target positioned after the ED, by adopting periodic conditions at the horizontal and vertical boundaries (like the EAMCC code); finally it computes the power load deposited on any single micro-area.

When electrons hit material surfaces, they can be back-scattered, so that their power can be re-distributed among the various tubes, and can also be reflected onto the downstream side of the GG.

The BACKSCAT code, developed at Consorzio RFX in the COMSOL® environment [12], can estimate the particle fluxes, by taking into account backscattering electrons impinging on the ED tubes. A 2D computational domain extends from the rear of the GG up to the end of the electron dump; like for EDAC, the particles coming from EAMCC are injected 20 mm downstream of the accelerator exit.

Two different models can be selected to account for the backscattering of electrons on the ED tubes. Model 1 is based on the work by Staub [13], used also in EAMCC with just few differences. In this model, the probability to be backscattered for an electron impinging on a pipe is expressed as a function of the electron energy and the incidence angle between particle trajectory and surface normal. This model accounts also for an energy loss of the primary electron during the backscattering process. Backscattered electrons possess a uniform angular distribution with respect to the impact point. The second model is based on the work by Thomas [14], which has a simpler formula for the backscattering probability: backscattered electrons keep all the energy they had before the impact (however this is not a strong approximation, since about 80% of electrons do not lose any energy).

As a preliminary check, BACKSCAT, with backscattering coefficient equal to zero, was compared to EDAC, yielding very similar results. The differences in the results of the two backscattering models can be interpreted in terms of the energy transfer during the impact. Since a richer physics is contained in model 1 it was selected as the reference for the following analyses.

The computation of the power deposited on the GG includes the aperture walls. A more accurate simulation was performed using the entire accelerator geometry, so that the particles travelling backward towards the source are subjected to the electrostatic and magnetic fields inside the accelerator. Another difference comes from the ratio between a circular aperture and the corresponding square. Figure 3 shows the trajectories of primary particles (in blue) and of backscattered electrons, followed even inside the accelerator.

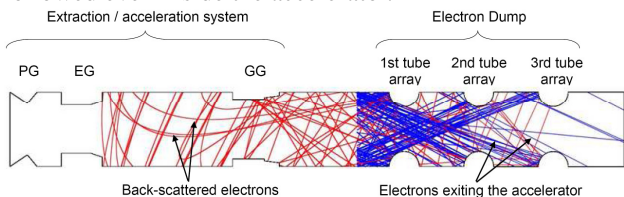


Figure 3: Simulation of electron backscattering in the whole accelerator geometry. Trajectories and heat loads..

Table 2: Power deposited on ED and GG iron plate.

GG iron plate	62	88
1 <sup>st</sup> tube array	221	257
2 <sup>nd</sup> tube array	185	206
3 <sup>rd</sup> tube array	176	183

Using BACKSCAT several cases have been studied, obtaining the optimal position of the tube arrays so as to

minimise the heat load on the GG as well as the transmitted power associated to electrons.

The total heat loads on the ED and on the GG iron plate are reported in Table 2; the trajectory of electrons and the distribution of power over the various surfaces are shown in Figure 4. Considering the possibility of out-of-reference scenarios (non optimal perveance), the heat loads are increased. These values are to be considered for dimensioning the cooling systems for the GG and ED [4].

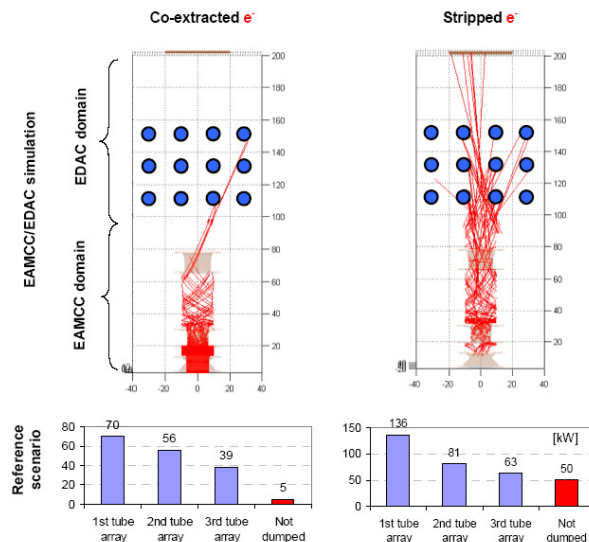


Figure 4: Electron heat loads dumped by the ED and transmitted out of the accelerator.

## REFERENCES

- [1] R. S. Hemsworth *et al.*, Rev. Sci. Instrum. 79 (2008) 02C109.
- [2] P. Sonato *et al.*, Fusion Eng. Des. 84 (2009) 269
- [3] P. Agostinetti *et al.*, AIP Conf. Proc. 1097 (2009) 325
- [4] P. Agostinetti *et al.*, in preparation
- [5] P. Agostinetti *et al.*, paper P2.11, 18th Int. Toki Conf. on Development of Physics and Technology of Stellarators /Heliotrons en route to Demo, Ceratopia Toki, Japan, 2008: [http://www.nifs.ac.jp/itc/itc18/upload/proceedings\\_upload/proc\\_P2-11\\_Agostinetti.pdf](http://www.nifs.ac.jp/itc/itc18/upload/proceedings_upload/proc_P2-11_Agostinetti.pdf).
- [6] G. Fubiani *et al.*, Phys. Rev. Special Topics Accelerators and Beams 11 (2008) 014202; G. Fubiani *et al.*, Phys. Rev. Special Topics Accelerators and Beams 12 (2009) 050102
- [7] J. Pamela. Rev. Sci. Instrum. 62 (1991) 1163; W. B. Hermannsfeld. SLAC report, SLAC-226 (1979); H.P.L. de Esch *et al.*, Fusion Eng. Des. 73 (2005) 329
- [8] OPERA Manual, Cobham, <http://www.vectorfields.com/>
- [9] ANSYS Manual, ANSYS Inc., <http://www.ansys.com/>
- [10] H.P.L. De Esch, R.S. Hemsworth, Fusion Eng. Des. 82 (2007) 723
- [11] G. Serianni *et al.*, 36th EPS Conference on Plasma Phys. Sofia, June 29 - July 3, 2009 ECA Vol.33E, P-4.171
- [12] COMSOL Manual, COMSOL AB <http://www.comsol.com/>
- [13] P. F. Staub, J. Phys. D: Appl. Phys. 27 (1994) 1533
- [14] E. W. Thomas, in Nuclear Fusion Special Issue "Data compendium for plasma surface interaction", cap 9 (1984)